International Journal of Coal Geology 77 (2009) 145–152

Contents lists available at ScienceDirect

International Journal of Coal Geology

journal homepage: www.elsevier.com/locate/ijcoalgeo

Modeling of coal bed methane (CBM) production and CO_2 sequestration in coal seams

Ekrem Ozdemir *

Izmir Institute of Technology, Chemical Engineering Department, 35420-Urla/Izmir, Turkey

ARTICLE INFO

Article history:
Received 30 April 2008
Received in revised form 28 August 2008
Accepted 7 September 2008
Available online 16 September 2008

Keywords:
CO_2
Sequestration
Coalbed methane
Modeling

ABSTRACT

A mathematical model was developed to predict the coal bed methane (CBM) production and carbon dioxide (CO_2) sequestration in a coal seam accounting for the coal seam properties. The model predictions showed that, for a CBM production and dewatering process, the pressure could be reduced from 15.17 MPa to 1.56 MPa and the gas saturation increased up to 50% in 30 years for a 5.4×10^5 m^2 of coal formation. For the CO_2 sequestration process, the model prediction showed that the CO_2 injection rate was first reduced and then slightly recovered over 3 to 13 years of injection, which was also evidenced by the actual in seam data. The model predictions indicated that the sweeping of the water in front of the CO_2 flood in the cleat porosity could be important on the loss of injectivity. Further model predictions suggested that the injection rate of CO_2 could be about 11×10^3 m^3 per day; the injected CO_2 would reach the production well, which was separated from the injection well by 826 m, in about 30 years. During this period, about 160×10^6 m^3 of CO_2 could be stored within a 21.4×10^5 m^2 of coal seam with a thickness of 3 m.

1. Introduction

Sequestration of carbon dioxide (CO_2) in unmineable coal seams has been proposed as one of the geologic strategies to mitigate increasing concentrations of CO_2 in the atmosphere (Reichle et al., 1999). Coal seam sequestration of CO_2 is particularly attractive in those cases where the coal contains large amounts of methane (CH_4) (White et al., 2005). In these cases, not only the CO_2 is stored in the coal seam in an adsorbed state but the coalbed methane (CBM) can also be produced to generate revenue that offsets the expense of sequestration. However, the mechanisms by which CO_2 moves through and dissipates into the coal matrix are not well understood.

Fig. 1 shows a schematic representation of the coal seam sequestration of CO_2. As depicted in the figure, the CO_2 is captured from the flue gases in a coal firing power plant and injected into the coal seam. Upon injection, CO_2 is expected to flow through the coal cleat system and be stored within the coal matrix (Ertekin et al., 1986). The following main questions need to be addressed to ensure a safe, cost-effective sequestration of large volumes of CO_2 in coal seams: How much CO_2 can be injected into a candidate coal seam?; How long would it take for the injection process?; What would the injection rate be?; How would the injected CO_2 distribute along the coal seam?; and Which parameters would affect most the injection process? These questions can be answered by an effective modeling of the sequestration process, which is essential both for an understanding of the complex interactions occurring during the CO_2 storage and for predicting the economic viability of the sequestration under the particular conditions of a given site.

Many commercial and research numerical models have been developed to simulate the CBM recovery processes (King and Ertekin, 1989a,b, 1995; King et al., 1986; Karacan, 2007; Kohler, 1999; Goktas, 1999; Almisned and Thrasher, 1995). In a three part survey, King and Ertekin (King and Ertekin, 1989a,b, 1995) reviewed the coalbed methane models which had been developed and published in the literature. They classified the models as: empirical, equilibrium, and non-equilibrium sorption models. The equilibrium models assume that the adsorption and desorption processes are so rapid that the kinetics of the process is negligible. In non-equilibrium models, the adsorption and desorption processes are time dependent and movement of the distributing component into and out of the coal matrix is retarded. These models have taken into account many of the factors important to coal seam sequestration including the dual porosity nature of coalbeds; multi-phase Darcy flow of gas and water in the natural fracture system; single component gas diffusion in the natural fracture system; adsorption and desorption processes of a single gas component on the coal surface; and coal matrix shrinkage due to gas desorption.

Sequestration of CO_2 in coal seams with concomitant recovery of CH_4 is a new technology that has been practiced in a few places but it is not well developed. Burlington Resources has performed enhanced coalbed methane recovery/CO_2 sequestration in deep unmineable coal seams in the San Juan Basin in New Mexico since 1996 (Stevens et al., 1999). The significance of the preliminary test results from the Allison unit was summarized as follows (Reeves, 2001):

(1) Injection of CO_2 began in 1995 at a rate of 141×10^3 m^3/day; since then, a loss of injectivity has reduced injection rates to about 85×10^3 m^3/day;
(2) A sharp increase in water production was observed immediately and during the initial 6-month period of CO_2 injection; and

* Tel.: +90 232 750 6685; fax: +90 232 750 6645.
E-mail address: ekremozdemir@iyte.edu.tr.

0166-5162/$ – see front matter © 2008 Elsevier B.V. All rights reserved.
doi:10.1016/j.coal.2008.09.003

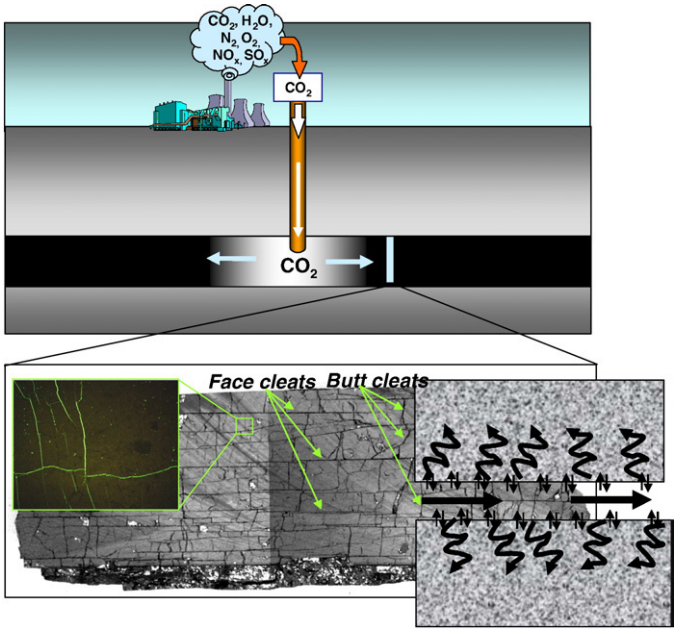

Fig. 1. A schematic representation of the coal seam sequestration of CO_2.

(3) Minimal breakthrough was observed during the 5 years of CO_2 injection.

It appears that the reduction in the injection rate could be due to closing of the cleat structure as a result of the coal swelling or to the reduction in the relative permeability in the presence of increasing water content in the cleat porosity. A better understanding of the mechanisms, both in the field and in the laboratory, will lead to improvements in the numerical simulators, and in the understanding of the complex processes occurring during the sequestration of CO_2 in coal seams. In order to relate the physical parameters to the CO_2 injection process, the transport of gases and water through the coal seam was modeled.

2. Modeling of fluid flow in coal seams

Coals are naturally fractured porous solids (Krevelen, 1961; Meyers, 1982). They are confined between a cap rock and floor strata, which are known to be impermeable to fluids (Smith et al., 1994). Most coal beds of importance to CO_2 sequestration are saturated with water and may contain coalbed methane (CBM). The seam pressure is near the hydrostatic pressure which increases with depth of the formation (Stevens et al., 1999). It has been suggested that the methane is adsorbed within the coal matrix and water resides in the cleat system (Kolesar et al., 1990).

The coal seams can be represented by either rectangular or cylindrical geometries for the modeling purposes. Because the thickness of the coal seam is much smaller than the drainage radius, (e.g. ~3 m vs. ~500 m) (Law, 1993), the cylindrical geometry was chosen in this study to represent the fluid flow in coal seams assuming that the cleat porosity and coal seam properties are evenly distributed along the reservoir. Fig. 2 illustrates the layout of a coal seam containing a well with a radius of r_w and its drainage radius, r_e,. In order to model the fluid flow within a coal seam, a differential volume element was considered at a distance of r from the well with a thickness of dr.

The following assumptions were considered in the modeling:

1. The reservoir is horizontal and its thickness is constant.
2. The porous medium is a continuum and its physical properties on the entire system can be represented by a control volume element.
3. The system is isothermal.
4. The flow in a coal seam is a two-phase flow including a water phase and a gas phase.
5. The free gas behaves as a real gas.
6. The fluid flow in the cleat porosity is a laminar flow due to larger pore sizes and governed by the Darcy's law while the flow in the coal matrix is a diffusional flow due to smaller pores and governed by Fick's Law.

By conducting a mass balance on a differential volume element in the cylindrical coordinates as illustrated in Fig. 2b, the governing equations for the flow of the gas phase and the water phase can be given as follows:

for CO_2 in the gas phase

$$-\frac{1}{r}\frac{\partial}{\partial r}\left\{r\left[\frac{y_1\alpha\alpha_1 kk_{rg}}{\mu_g B_g}\frac{\partial P_g}{\partial r}+y_1 D_a\frac{\partial}{\partial r}\left(\frac{S_g}{B_g}\right)+R_{SW1}\frac{\alpha kk_{rw}}{\mu_w B_w}\frac{\partial(P_g-P_{cgw})}{\partial r}\right]\right\} \pm(q_{ai})_1=\frac{\partial}{\partial t}\left(\frac{y_1\phi S_g}{B_g}+R_{SW1}\frac{\phi(1-S_g)}{\alpha_1 B_w}\right) \quad (1)$$

for CH_4 in the gas phase

$$-\frac{1}{r}\frac{\partial}{\partial r}\left\{r\left[\frac{(1-y_1)\alpha\alpha_1 kk_{rg}}{\mu_g B_g}\frac{\partial P_g}{\partial r}+(1-y_1)D_a\frac{\partial}{\partial r}\left(\frac{S_g}{B_g}\right)+R_{SW2}\frac{\alpha kk_{rw}}{\mu_w B_w}\frac{\partial(P_g-P_{cgw})}{\partial r}\right]\right\} \pm(q_{ai})_2=\frac{\partial}{\partial t}\left(\frac{(1-y_1)\phi S_g}{B_g}+R_{SW2}\frac{\phi(1-s_g)}{\alpha_1 B_w}\right) \quad (2)$$

for the water phase

$$-\frac{1}{r}\frac{\partial}{\partial r}\left(r\frac{\alpha kk_{rw}}{\mu_w B_w}\frac{\partial(P_g-P_{cgw})}{\partial r}\right)\pm q_{wi}=\frac{\partial}{\partial t}\left(\frac{\phi(1-S_g)}{\alpha_1 B_w}\right). \quad (3)$$

Definition of each symbol can be found in the nomenclature. And, the detailed derivations of the model equations, the boundary conditions, and the computer code for the solution are given in Ozdemir (2004).

The governing differential equations representing the simultaneous flow of the gas and the water phases in a coal seam can be coupled with a non-equilibrium source term as:

$$(q_{ai})_i=-\frac{A}{V}D_i\frac{RT_{sc}}{P_{sc}}\frac{\partial C_i}{\partial r}\Big|_{r=Z_c} \quad (4)$$

where the transport of gases into and out of the coal matrix can be calculated from the concentration profile within the coal matrix, which is a function of the space and time, $C_i=C_i(r,t)$, and it can be obtained by solving Eq. (5) employing the initial and the boundary conditions.

$$\frac{\partial}{\partial r}\left(rD_i\frac{\partial C_i}{\partial r}\right)=\frac{\partial C_i}{\partial t}. \quad (5)$$

Note that similar (r, θ, z) notations was used to represent the coal matrix since after closely investigating the cross-section of the coal seam as shown in Fig. 1, the coal matrix is divided into rectangular, cylindrical, and rhombic types of shapes surrounded by the face and butt cleats. Because the face cleats are longer than the butt cleats (Laubach et al., 1998), the coal matrix was considered to be a cylindrical shape parallel to the face cleats.

2.1. Dependence of coefficients in the governing equations on pressure and saturation

In most instances, actual in-seam data are not available. In these circumstances, correlations are used to compute in the modeling. Parameters such as porosity (Puri et al., 1991), absolute permeability

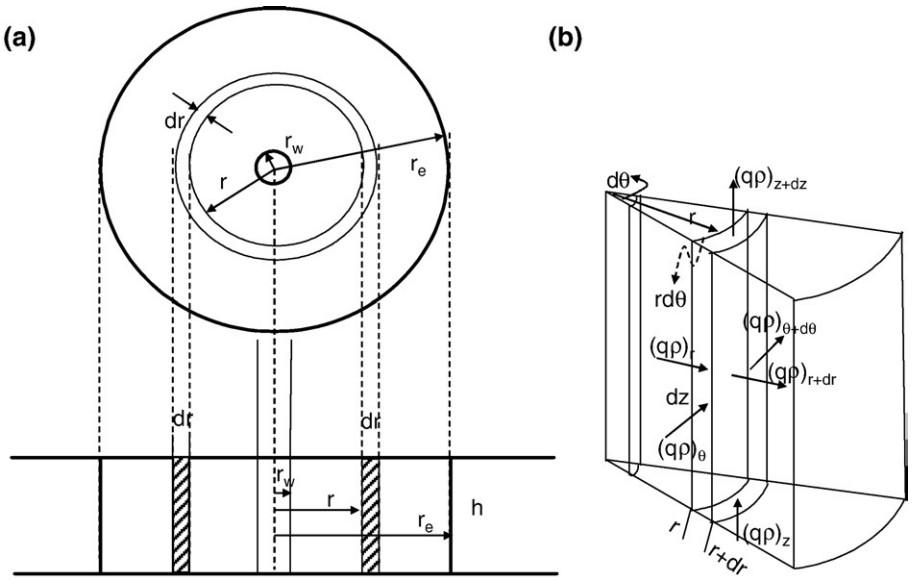

Fig. 2. The layout for a coal seam.

(Durucan and Edwards, 1986), relative permeability (Crichlow, 1977), viscosity (Craft et al., 1991), formation volume factor (McCain, 1988), capillary pressure (Crichlow, 1977), and compressibility factor (Dake, 1978) are all pressure and saturation dependent, and these relationships are given in the indicated references and in Ozdemir (2004).

3. Solution of the governing equations

The governing equations, Eqs. (1)–(4), can be solved analytically for only certain simplified conditions. Instead, because these equations are quite complex and non-linear, a numerical solution has to be implemented. Therefore, the governing differential equations were solved by using the solver in the Athena Visual Workbench Software Package® (Athena, 2002). Athena is a computational tool that allows programmers to solve complex systems of equations. The package uses the finite-difference approximation to transform the governing partial differential equations describing the flow of gas and water in a coal seam into algebraic finite-difference equations. The advantages of using Athena are that it is faster and saves time. It can solve the non-linear systems of equations once they are organized as input variables. The disadvantages using Athena are that the Athena can solve only one-dimensional un-steady state equations, and the wells at the external boundary could not be defined. The numerical solution for the governing equations was implemented by superimposing a finite-difference grid over the idealized coal seam. The finite-difference solution then produced the values of pressure and saturation at discrete points in the coal seam and calculated the flow rates and cumulative productions for the gas and the water phases during the CBM production or CO_2 injection process.

Table 1
Physical parameters used in the model

	CBM production	CO_2 injection	
Reservoir area	5.4×10^5	21.4×10^5	m^2
Average reservoir depth	975.36	975.36	m
Formation thickness	3.05	3.05	m
Effective porosity	2.00	2.00	%
Absolute permeability	2.00	2.00	md
Formation compressibility	0.15×10^{-3}	0.15×10^{-3}	MPa^{-1}
Coal density	1.36	1.36	g/cm^3
Formation temperature	68.10	68.10	°C
Initial formation pressure	15.17	3.45	MPa
Initial water saturation	0.95	0.60	Fraction
Well radius	8.89	8.89	cm
Wellbore pressure	0.17	15.17	MPa
Cleat spacing	1.31	1.31	cm
Micropore diffusion coefficient	0.19×10^{-6}	0.19×10^{-6}	m^2/day
Sorption time constant	231.46	231.46	day

4. Results and discussion

4.1. Validation of the two-phase fluid flow model

The compositional two-phase fluid flow model developed in this study was tested against a two-phase single component model developed by Sung (Sung, 1987; Sung et al., 2000). The Sung's model has also been used by others to test their models (Kohler, 1999; Manik, 1999). Both models were run using the same properties of a reservoir system as depicted in Table 1, Figs. 3 and 4. The comparison was made for the four sets of data of simulation runs when either the source term was included or it was excluded. The agreement between the two models was better than expected. These numerical simulation exercises indicated that the compositional two-phase model developed in this study was more efficient as being faster and better optimized than that of the Sung's two-phase model. Therefore, the present model was considered to be used to relate the parameters involving the gas and water transport in a coal seam to the CBM production and the CO_2 sequestration processes.

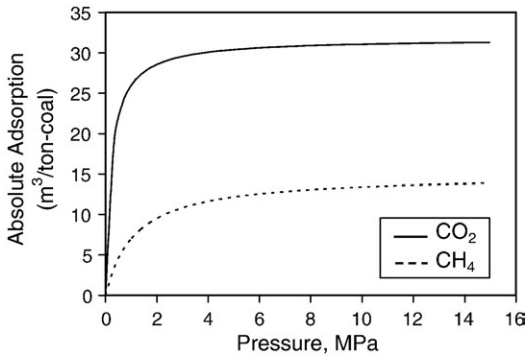

Fig. 3. Adsorption isotherms of CO_2 and CH_4 on the coal used in the models.

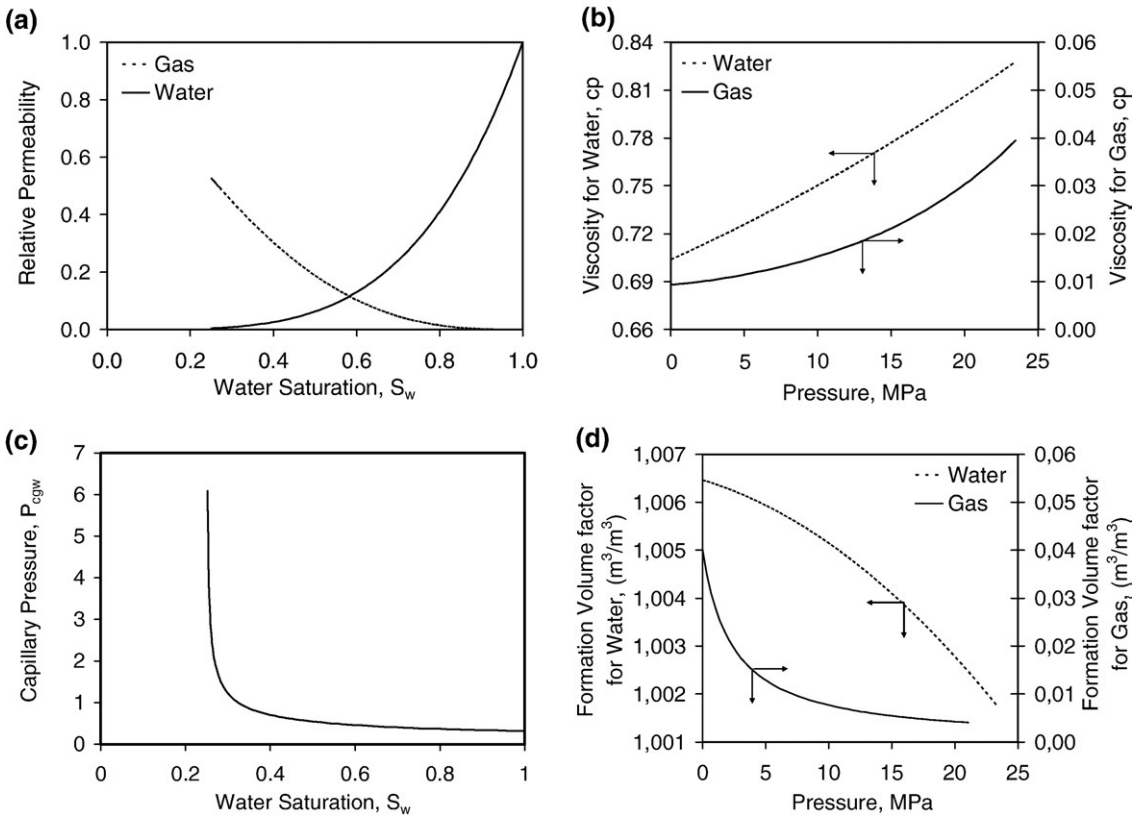

Fig. 4. The Parameters for gas and water phases used in the models (a) relative permeability (b) viscosity (c) capillary pressure, and (d) formation volume factor.

4.2. Model predictions of CBM production: dewatering and degasification of a coal seam

Because about 90% of the gas storage occurs within the coal matrix, any methane and water occupying the coal porosity decrease the adsorption capacity and inhibits the diffusion within the coal matrix. Therefore, the first step in coal seam sequestration is to drain the water and recover adsorbed methane. Thus, a series of computer runs were performed to illustrate the methane and water production from a coal seam.

Fig. 5 shows the effect of bottomhole pressure selected for the internal boundary condition on the gas production rate, the water production rate, and the cumulative productions. These data suggest that, typically, there are three stages in coal dewatering/degasification process (McKee and Bumb, 1987). At stage I, which corresponds to the first year in the figure, a huge amount of water is produced at the initial drainage because water initially occupies the cleat porosity in the reservoir, which controls the flow to the production well. At this stage, the relative permeability for water is high. As the water production continues, the hydrostatic pressure decreases, which result in the adsorbed methane to desorb and enter into the cleat porosity. The gas production rate is low and it increases as the water continues to be removed from the cleat system. Thus, the relative permeability to water decreases while the relative permeability to the gas increases. As can be seen in the figure, at the end of about 2nd year, most of the water is pumped-off and the gas production rate reached at its maximum. At stage II, which corresponds to the second and third year in Fig. 5, the gas production rate reaches at its maximum while the water production rate is considerably reduced. At this stage, the reservoir flow condition is almost stabilized until the beginning of the third stage. At stage III, which corresponds to the fifth year and thereafter in Fig. 5, the gas production rate is to decline. At this stage, the water production is low or negligible. Also, at this stage, both of the relative permeabilities to gas and water change very little.

As shown in Fig. 5a and c, the gas production rate and the cumulative gas production are the highest when the bottomhole pressure is specified at its lowest level, i.e. near the atmospheric pressure. When the bottomhole pressure specification is increased, the production rate and the cumulative production are to decrease. Similar results were obtained for the water production rate and cumulative water production. Here, the water production rate in Fig. 5b was given for the first 5 years to better display the data. However, the cumulative water produced did not change significantly unless the specified bottomhole pressure is near the initial pressure at the in-seam condition. The intension here is to withdraw the gas and water from the coal seam as quickly as possible to be able to inject the CO_2 at the earliest time possible. Therefore, the bottomhole pressure should be selected as low as possible.

The constant flow rate specification could also be made as the internal boundary condition at the production well. The results indicated that the greater the specified total production rate the greater the gas production rate could be obtained. On the other hand, the effect of the total production rate specification was not significant on the production rate for the water phase. The bottomhole pressure was nearly the initial in-seam pressure for the low production rate specification of 70 m^3/day as shown in Fig. 6. As the total production rate at the well increased to 706 m^3/day, the bottomhole pressure could be reduced to near the atmospheric pressure after about 27 years of production. The low in-seam pressure could be advantageous because the higher injection rate of CO_2 could be achieved.

The model can also predict the pressure variations and gas saturation in the specified coal seam. Fig. 7a shows the pressure distribution along the coal seam and in the vicinity of the production well during the dewatering and degasification process. Here, the

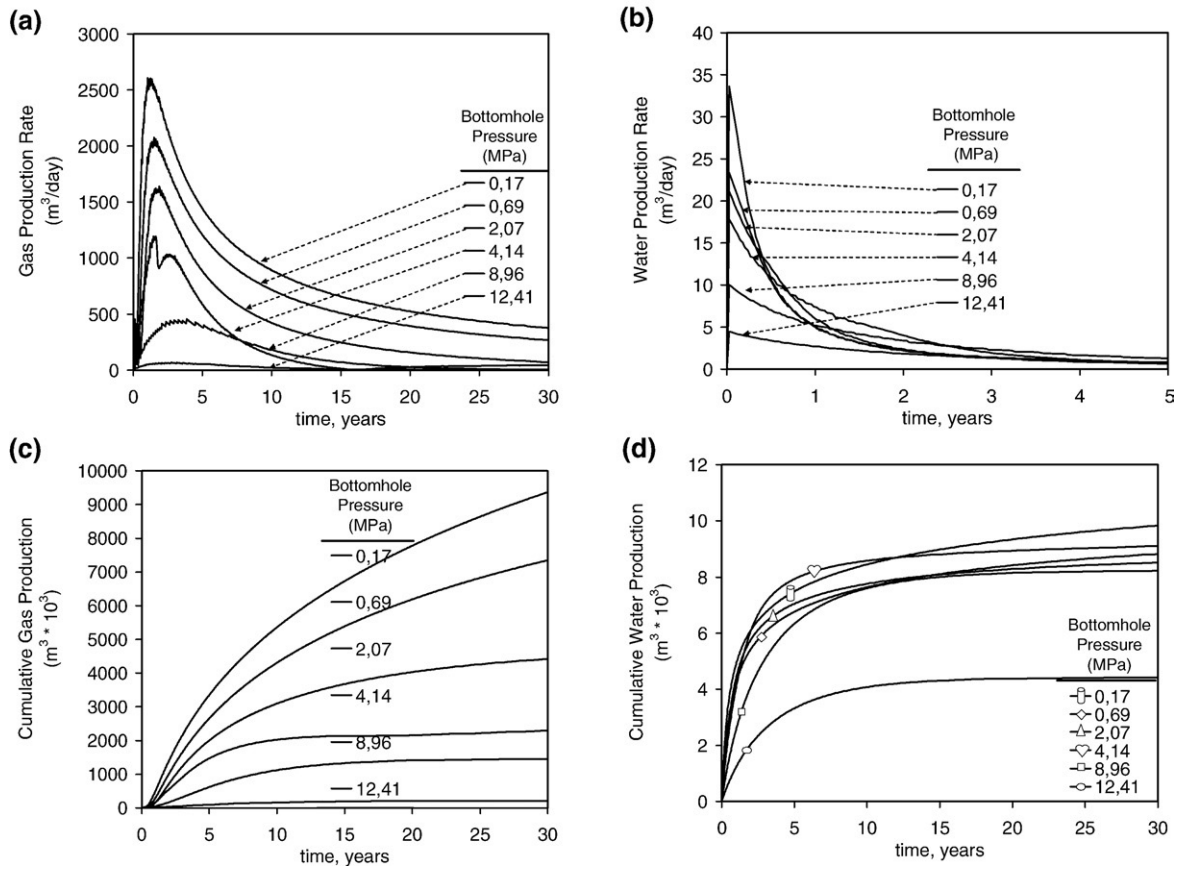

Fig. 5. Effect of bottomhole pressure specification at the internal boundary on the gas and water production rates and the cumulative productions (a) gas production rate (b) water production rate (c) cumulative production rate for gas (d) cumulative production rate for water.

pressure at the well was specified to be near atmospheric (0.17 MPa) for an aggressive dewatering and degasification of the coal seam and to achieve maximum production rates. As can be seen, the pressure decline is more noticeable at the vicinity of the production well. Because the cleat porosity was occupied by the water and the production of water reduces the hydrostatic pressure, the pressure decreases along the coal seam over time. As a result of the pressure decline, the adsorbed methane starts to desorb and fill the cleat porosity. The decrease in the pressure and the desorption of methane result in the gas saturation, as expected, to increase in the cleat system as shown in Fig. 7b. The gas saturation could only be increased up to 70% near the well and 50% away from the well over a 30 year period of degasification and dewatering process. At this time, the pressure could decrease up to 1.56 MPa.

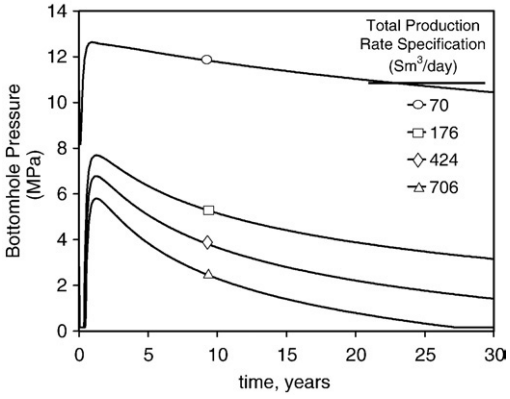

Fig. 6. Bottomhole pressure for the case of constant total flow rate.

At the specified reservoir conditions, it seems that the pressure could only be reduced to about 1.56 MPa and the gas saturation increased up to 50% at the end of 30 years of degasification process. Delaying the injection process for 30 years may not be practical for the degasification and dewatering of a coal seam before starting the CO_2 injection. For instance, in 5 years of production, the gas saturation could reach up to 40% and the pressure could be reduced up to 3.4 MPa. On the other hand, it seems that the length of the dewatering and degasification process is controlled by the physical properties of the coal seam and project development parameters. For instance, fracturing the coal seam and a closely spaced well configuration could significantly reduce the time for the dewatering and degasification processes of a coal seam.

4.3. Model predictions of CO_2 sequestration in a coal seam

The previously defined layout for the dewatering and degasification of a coal seam was rearranged for the CO_2 injection process. In this configuration, one of the wells at the center was considered for the CO_2 injection. The default reservoir parameters used in these simulations are listed in Table 1. Here, the reservoir size was taken to be 826 m, which is the double in size of the field that was studied for the degasification and dewatering process. The initial gas saturation and in-seam pressure were taken to be 0.4 and 3.4 MPa, respectively, considering a 5 year of dewatering and degasification process. The pressure, the mole fraction of CO_2, and the gas saturation at the injection well were set to be 15.2 MPa, 1.0, and 1.0, respectively. The external boundary was considered to open to the atmosphere through the production wells. Because Athena is not capable of

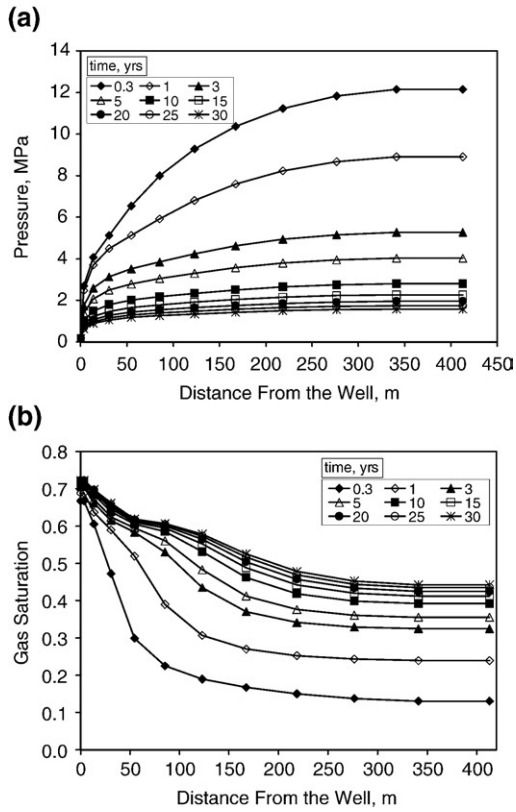

Fig. 7. (a) Pressure distribution and (b) gas saturation during the dewatering and degasification of a coal seam.

representing the production wells at the external boundary, the flow rates at the production well could not be reported. Instead, the CO_2 injection rates, the cumulative injected CO_2, the CO_2 composition, the pressure, and the gas saturation profiles along the coal seam were reported. The external boundary was set to shut-in in the model runs when the mole fraction of CO_2 reaches to the value of 0.5 at the exit. The model runs were continued until the in-seam pressure reaches closer to the initial in-situ pressure.

Fig. 8 shows the CO_2 injection rate, the cumulative injected CO_2, the mole fraction of the CO_2 in the gas phase, the pressure distribution, and the gas saturation along the coal seam over time. As shown in Fig. 8a, a 12×10^3 m^3 of CO_2 per day could be injected into the specified coal seam, where the injection rate decreases slightly to about 9×10^3 m^3/day initially and then recovers in about 10 years, reaching a steady injection rates of about 11×10^3 m^3/day. After the external boundary was shut-in, the injection rate started to decrease for the next 5 to 8 years until the injection process is complete. In 40 years of CO_2 injection, about 160×10^6 m^3 of CO_2 could be stored within a 21.4×10^5 m^2 of coal seam with a thickness of 3 m.

Fig. 8b shows the mole fraction of CO_2 in the gas phase along the coal seam. It seems that the injected CO_2 flows through the coal seam towards the production well at the external boundary with a moving front. The mole fraction of CO_2 behind the moving front is about unity whereas there is no CO_2 after the moving front. The mole fraction decreases sharply at the moving front. The CO_2 breakthrough could be seen at about 36 years for the present configuration.

Fig. 8c shows the pressure profiles during the CO_2 injection. As can be seen from the figure, almost linear pressure profiles were established between the injection and the production wells at the external boundary until the CO_2 breakthrough was observed. After the production wells were shut-in, the pressure was steadily build-up and reached closer to the initial in-situ pressures after 43 years.

Fig. 8d shows the gas saturation profiles within the coal seam. The gas saturation is about 1.0 near the injection well and decreases along the coal seam. The most interesting finding in these simulation results is that the gas saturation decreases significantly near the moving front (see Fig. 8b). Especially, the gas saturation is seen to decrease below the initially specified level in the first year of injection. For the

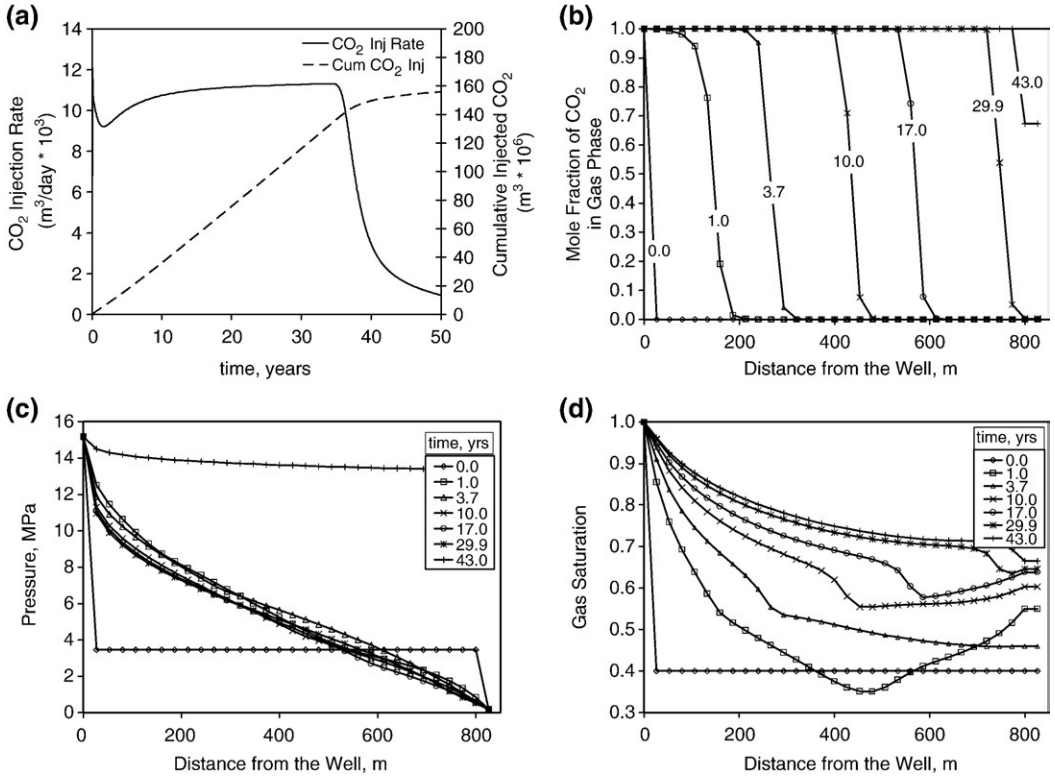

Fig. 8. CO_2 injection in coal seam including the source term (a) CO_2 injection rate and the cumulative injected CO_2, (b) mole fraction of CO_2 in the gas phase (c) pressure (d) gas saturation.

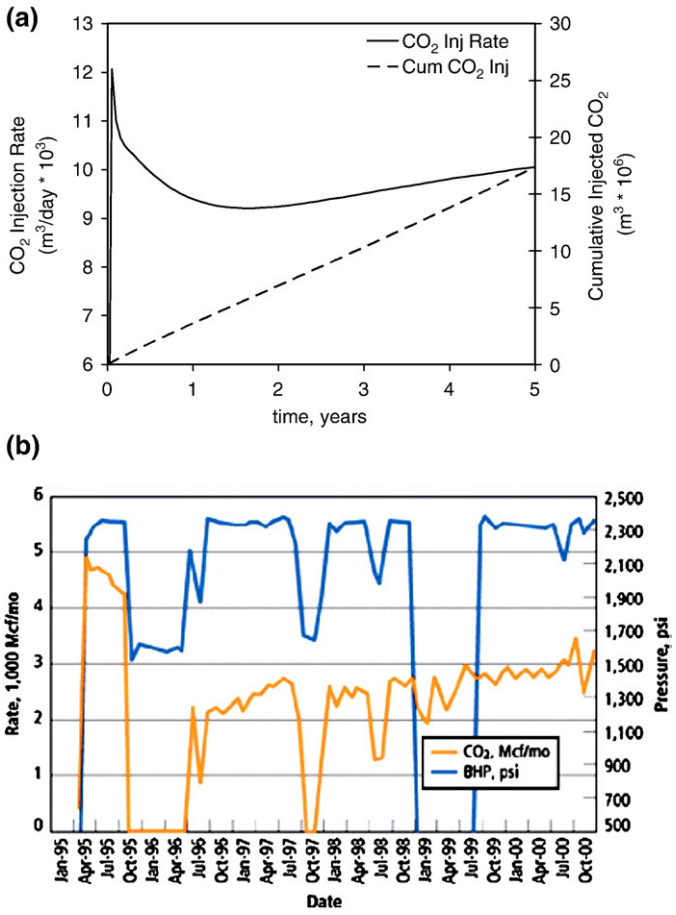

Fig. 9. CO_2 injection in coal seams: (a) prediction by the present hypothetical model, and (b) an actual in-seam data (Reeves, 2001).

following years, a sudden decrease in the gas saturation is observed with the moving front indicating that the CO_2 replaces the water and pushes it toward the production well at the external boundary. This may be one of the main causes for the loss of injectivity during the beginning of injection process as shown in Fig. 8a.

4.4. Model prediction and actual in-seam data

An actual in-seam data for a CO_2 injection in San Juan Basin was reported by Reeves (2001), as shown in Fig. 9b. The figure shows the CO_2 injection rate while keeping the bottomhole pressure constant at about 15.6 MPa. Although there are irregularities during the injection, the general trend in actual in-seam data is that the CO_2 injection rate was first reduced throughout the first year and then started slightly to increase over 2 to 5 years of injection. A similar trend was observed with the present hypothetical modeling. As shown in Fig. 9a, the CO_2 injection rate estimated by the model was first reduced during the first year and then started slightly to increase for the next 2 to 5 years of injection. The decrease in the injection rate could be due to the volumetric changes occurring during the adsorption/desorption processes on coal. As illustrated in Fig. 8d, the decrease in the injection rate could also be due to the flooding of the water in the cleat porosity extracted by the CO_2.

5. Conclusion

Dewatering, degasification, and injection of CO_2 in a coal seam are complicated processes. The model runs performed to illustrate the CBM and water production from a coal seam suggest that the gas saturation could increase up to 50% and the pressure could decrease down to 1.56 MPa in 30 years of the degasification process. These values clearly suggest that most of the *in-situ* water and the CBM, (as shown in Fig. 3), would still be left behind in the coal seam. Although the presence of the moisture and adsorbed methane decreases the CO_2 storage capacity of a coal (Joubert et al., 1974), the injected CO_2 could replace the remained moisture and methane as reported by Reznik et al. (1984). As evidenced by the actual in-seam data (Reeves, 2001) and by the present hypothetical model, the CO_2 injection rate decreases initially and starts to recover over the next several years of injection. The decrease in the injection rate could be related to the swelling/shrinkage of the coal upon the CO_2 sorption/CH_4 and water desorption processes. Removing the moisture and methane from the coal has been shown to shrink the coal (Suuberg et al., 1993; Ozdemir et al., 2004), and readsorption of CO_2 was shown to swell the coal to a similar extend (Ozdemir, 2004; Ozdemir et al., 2004). In addition, as predicted from the present model, the decrease in the injection rate could also be related to the flooding of the water in the cleat porosity. The injected CO_2 has the capability of sweeping the water retained in the cleat porosity with a drying effect (Iwai et al., 2000) and push it to the external boundary reducing the flow rate to the gases. Therefore, it can be suggested that the water banking and the relative permeability effects may have been a contributing, or even a major, factor causing the observed field data.

Nomenclature

A	area perpendicular to the flow	m^2
B_g	formation volume factor for the gas phase	m^3/Sm^3
B_w	formation volume factor for the water phase	m^3/Sm^3
C_i	concentration within the coal matrix	mol/m^3
D_a	macropore diffusion coefficient	m^2/day
D_i	micropore diffusion coefficient	m^2/day
K	absolute permeability	md
k_g	permeability to gas phase	md
k_{rg}	relative permeability for gas phase	fraction
k_{rw}	relative permeability for water phase	fraction
P	pressure	MPa
P_{cgw}	capillary pressure between gas and water phases	MPa
P_{well}	pressure at the well-bore	MPa
q_{ai}	adsorption/desorption (source) term for gas	$Sm^3/day/m^3$
q_{wi}	adsorption/desorption (source) term for water	$Sm^3/day/m^3$
r_e	equivalent well block radius	m
R_{sw}	dissolved gas in water	Sm^3/Sm^3
S_g	gas saturation	fraction
T	temperature	K
y_i	mole fraction for ith component	fraction
Z_c	the half of the cleat spacing	m

Greek Letters

A	unit conversion factor for permeability	$(m^3/day)cP/m^2/(MPa/m)/md$
α_1	unit conversion factor	m^3/Sm^3
μ_g	viscosity of the gas phase	cP
μ_w	viscosity of the water phase	cP
ρ_w	density for water	g/cm^3

Acknowledgments

The author is grateful to Dr. Karl Schroeder and Dr. Curt White of the Department of Energy - National Energy Technology Laboratory (DOE-NETL), Dr. Robert M. Enick and Dr. Badie I. Morsi of the University of Pittsburgh-Chemical Engineering Department, and Dr. Turgay Ertekin and Dr. Ozgen Karacan of the Pennsylvania State University-Petroleum Engineering Department for their helpful discussions.

References

Almisned, O.A., Thrasher, R.L., 1995. Simulation of coalbed methane enhanced recovery using gas potential and a new saturation equation. Intergas'95, University of Alabama, Tuscaloosa, Alabama, May 15-19.

Athena, 2002. Athena Visual Workbench: Modeling, Optimization and Nonlinear Parameter Estimation for Scientists and Engineers. http://www.athenavisual.com/.
Craft, B.C., Hawkins, M.F., Terry, R.E., 1991. Applied Petroleum Reservoir Engineering. Prentice Hall, Englewood Cliffs, New Jersey.
Crichlow, H.B., 1977. Modern Reservoir Engineering — A Simulation Approach. Prentice Hall, Englewood Cliffs, New Jersey.
Dake, L.P., 1978. Fundamentals of Reservoir Engineering. Elsevier, New York.
Durucan, S., Edwards, J.S., 1986. The effects of stress and fracturing on permeability of coal. Min. Sci. Technol. 3, 205–216.
Ertekin, T., King, G.R., Schwerer, F.C., 1986. Dynamic gas slippage: a unique dual-mechanism approach to the flow of gas in tight formations. SPE Form. Eval. 43–52.
Goktas, B., 1999. Development and Application of a Local Grid Refinement Technique for Accurate Representation of Cavity-Completed Wells in Reservoir Simulators. Ph.D. Thesis, Pennsylvania State Univ., State College, PA.
Iwai, Y., Murozono, T., Koujina, Y., Arai, Y., Sakanishi, K., 2000. Physical properties of low rank coals dried with supercritical carbon dioxide. J. Supercrit. Fluids 18, 73–79.
Joubert, J.I., Grein, C.T., Bienstock, D., 1974. Effect of moisture on the methane capacity of american coals. Fuel 53, 186–190.
Karacan, C.O., 2007. Development and application of reservoir models and artificial neural networks for optimizing ventilation air requirements in development mining of coal seams. Int. J. Coal Geol. 72, 221–239.
King, G.R., Ertekin, T.M., 1989a. A survey of mathematical models related to methane production from coal seams, part I: empirical & equilibrium sorption models. Proceedings of 1989 Coalbed Methane Symposium, Tuscaloosa, April 17-20.
King, G.R., Ertekin, T.M., 1989b. A survey of mathematical models related to methane production from coal seams, part II: non-equilibrium sorption models. Proceedings of 1989 Coalbed Methane Symposium, Tuscaloosa, April 17-20.
King, G.R., and Ertekin, T.M., 1995. State-of-the-Art for Unconventional Gas Recovery, Part II: Recent Developments (1989-1994). SPE 29575, 289-312.
King, G.R., Ertekin, T., Schwerer, F.C., 1986. Numerical simulation of the transient behavior of coal-seam degasification wells. SPE Form. Eval. 165–183.
Kohler, T.E., 1999. Development and Application of a Compositional Coalbed Methane Production Model. Ph.D. Thesis, Pennsylvania State Univ. State College, PA.
Kolesar, J.E., Ertekin, T., Obut, S.T., 1990. The unsteady-state nature of sorption and diffusion phenomena in the micropore structure of coal: part I — theory and mathematical formulation. SPE Form. Eval. 81–88.
Krevelen, D.W. van, 1961. Coal: Topology-Chemistry-Physics-Constitution. Elsevier, New York.
Laubach, S.E., Marrett, R.A., Olson, J.E., Scott, A.R., 1998. Characteristics and origins of coal cleat — a review. Int. J. Coal Geol. 35, 175–207.
Law, B.E., 1993. The relationship between coal rank and cleat spacing: implications for the prediction of permeability in coal. Proc. Int. Coalbed Methane Symp. II 435–442.
Manik, J., 1999. Compositional Modeling of Enhanced Coalbed Methane Recovery. Ph.D. Dissertation, Pennsylvania State Univ., State College, PA.
McCain, W.D., 1988. The Properties of Petroleum Fluids, 2nd ed. Pennwell Publishing Co., Tulsa, OK.
McKee, C.R., Bumb, A.C., 1987. Flow-testing coalbed methane production wells in the presence of water and gas. SPE Form. Eval. 599–608.
Meyers, R.A., 1982. Coal Structure. Academic Press, New York.
Ozdemir, E., 2004. Chemistry of the Adsorption of Carbon Dioxide by Argonne Premium Coals and a Model to Simulate CO_2 Sequestration in Coal Seams. PhD. Dissertation. University of Pittsburgh. (http://etd.library.pitt.edu/ETD/available/etd-06182004-101850/unrestricted/Ozdemir-Hope-Final.pdf).
Ozdemir, E., Schroeder, K., Morsi, B.I., 2004. CO_2 adsorption capacity of Argonne premium coals. Fuel 83, 1085–1094.
Puri, R., Evanoff, J.C., Brugler, M.L., 1991. Measurement of coal cleat porosity and relative permeability characteristics. SPE Gas Technol. Symp. 93–104.
Reeves, S., 2001. Geologic sequestration of CO_2 in deep, unmineable coalbeds: an integrated research and commercial-scale field demonstration project. First National Carbon Sequestration Conference, U.S.DOE/NETL, pp. 1–12.
Reichle, D., Houghton, J., Kane, B., and Ekmann, J. et al., 1999. Carbon Sequestration: Research and Development. U.S. DOE report.
Reznik, A.A., Singh, P.K., Foley, W.L., 1984. An analysis of the effect of CO_2 injection on the recovery of in-situ methane from bituminous coal: an experimental simulation. SPE J. 521–528.
Smith, K.L., Smoot, L.D., Fletcher, T.H., Pugmire, R.J., 1994. The Structure and Reaction Processes of Coal. Plenium Press, New York.
Stevens, S.H., Kuuskraa, V.A., Spector, D., Riemer, P., 1999. CO_2 Sequestration in Deep Coal Seams: Pilot Results and Worldwide Potential. IEA Greenhouse Gas R&D Programme.
Sung, W., 1987. Development, Testing and Application of a Multi-Well Numerical Coal Seam Degasification Simulator, Ph.D. Dissertation, Pennsylvania State Univ., State College, PA.
Sung, W.M., Huh, D.G., Ryu, B.J., Lee, H.S., 2000. Development and application of gas hydrate reservoir simulator based on depressurizing mechanism. Korean J. Chem. Eng. 17, 344–350.
Suuberg, E.M., Otake, Y., Yun, Y., Deevil, S.C., 1993. Role of moisture in coal structure and the effects of drying upon the accessibility of coal structure. Energy Fuels 7, 384–392.
White, C.M., Smith, D.H., Jones, K.L., Goodman, A.L., Jikich, S.A., LaCount, R.B., DuBose, S.B., Ozdemir, E., Morsi, B.I., Shroeder, K.T., 2005. Sequestration of carbon dioxide in coal with enhanced coalbed methane recovery — a review. Energy Fuels 19, 559–724.